Progress in line-shape modeling of K-shell transitions in warm dense titanium plasmas

2009 J. Phys. A: Math. Theor. 42 214056

(http://iopscience.iop.org/1751-8121/42/21/214056)

IOP PUBLISHING JOURNAL OF PHYSICS A: MATHEMATICAL AND THEORETICAL

J. Phys. A: Math. Theor. **42** (2009) 214056 (10pp) doi:10.1088/1751-8113/42/21/214056

Progress in line-shape modeling of K-shell transitions in warm dense titanium plasmas

E Stambulchik[1], V Bernshtam[1], L Weingarten[1], E Kroupp[1], D Fisher[1], Y Maron[1], U Zastrau[2], I Uschmann[2], F Zamponi[2,6], E Förster[2], A Sengebusch[3], H Reinholz[3,4], G Röpke[3] and Yu Ralchenko[5]

[1] Faculty of Physics, Weizmann Institute of Science, Rehovot 76100, Israel
[2] Institute of Optics and Quantum Electronics, Friedrich-Schiller University, 07743 Jena, Germany
[3] Institute of Physics, University of Rostock, D-18051 Rostock, Germany
[4] School of Physics, University of Western Australia, Crawley, 6009 WA, Australia
[5] National Institute of Standards and Technology, Gaithersburg, MD 20899-8422, USA

E-mail: Evgeny.Stambulchik@weizmann.ac.il

Received 21 October 2008
Published 8 May 2009
Online at stacks.iop.org/JPhysA/42/214056

Abstract

Modeling of x-ray spectra emitted from a solid-density strongly coupled plasma formed in short-duration, high-power laser–matter interactions represents a highly challenging task due to extreme conditions found in these experiments. In this paper we present recent progress in the modeling and analysis of $K\alpha$ emission from solid-density laser-produced titanium plasmas. The self-consistent modeling is based on collisional-radiative calculations that comprise many different processes and effects, such as satellite formation and blending, plasma polarization, Stark broadening, solid-density quantum effects and self-absorption. A rather strong dependence of the $K\alpha$ shape on the bulk electron temperature is observed. Preliminary analysis of recently obtained experimental data shows a great utility of the calculations, allowing for inferring a temperature distribution of the bulk electrons from a single-shot measurement.

PACS numbers: 52.38.−r, 32.70.Jz, 52.50.Jm, 52.70.−m

1. Introduction

Measurements of characteristic inner-shell $K\alpha$ emission have proven to be powerful diagnostics for solid-state-density plasmas formed in interactions of intense particle [1–3] and laser [4–8] beams with matter. Such transitions are possible because of the inner-shell vacancies

[6] Present address: Max Born Institute, Max-Born-Strasse 2A, 12489 Berlin, Germany.

('holes') created either by the energetic particles of the beam or by the electrons accelerated to relativistic energies by the strong laser fields.

In this paper we focus on the spectroscopic modeling of laser-produced titanium plasmas, therefore from now on we assume energetic electrons as the primary source of the inner-hole production. These energetic fast electrons are produced in a thin high-temperature plasma layer at the front surface of the target, where the actual interaction between the laser radiation and the matter takes place. The depth of this hot plasma (<100 nm) is determined by the skin effect. Deeper layers of the target material have rather moderate temperatures, of tens of eV or even less. At solid density, such a highly coupled plasma is typically referred to as a 'warm dense matter' (WDM). Because of the high density, only short-wavelength radiation may escape the inner parts of the target; it is due to this reason that the inner-shell x-ray emission is an important instrument to yield valuable information about such plasmas.

The modeling of the radiation properties of WDM poses several challenges. Because of significant coupling, density effects (e.g., continuum lowering, collectivized electrons, degeneracy effects) become of paramount importance; they cannot be treated as mere corrections, as usually done for weakly coupled plasmas. Also, the presence of the two electron fractions (the bulk and the fast ones), differing in energies by several orders of magnitude, results in an essentially non-equilibrium state. Furthermore, in practical terms, these two very different electron distributions complicate the collisional-radiative calculations significantly, since all atomic processes involving free electrons need to be tabulated over a very wide range of the electron energies.

2. Atomic and plasma modeling

The electronic configuration of atomic Ti in the ground state is $1s^2 2s^2 2p^6 3s^2 3p^6 3d^2 4s^2$. However, in the bulk titanium delocalized quasi-free electrons have to be taken into account. Even in the low-temperature limit four outer electrons (in the 3d and 4s orbitals) are collectivized (see [9] for details). We also obtained a similar result using the `INFERNO` average atom model [10], which gives $\langle Z_i \rangle \approx 4$. Therefore, the lowest charge state that we take into account is argon-like Ti v with the electron density in the zero-temperature limit $n_e = 4n_i$, where $n_i \approx 5.66 \times 10^{22}$ cm^{-3} is the ion-particle density in the solid-state titanium.

For the calculations we employed a collisional-radiative (CR) code [11], in which the following processes were included: spontaneous radiative decay, autoionization (including the Auger effect), electron-impact collisional processes (excitation, de-excitation and ionization), recombination (radiative, three-body and dielectronic). Five charge states, from Ar-like to Si-like titanium, were included. All atomic data for the present calculations (i.e., energy levels, radiative and autoionization rates, and cross-sections for all processes involving free electrons in the initial state) were calculated using the Flexible Atomic Code (FAC) [12].

In addition to the ground state of each charge state included, accounted were a number of excited states up to the ionization limit. These states are heavily affected by the plasma surrounding that causes lowering of the ionization potential. This lowering was calculated based on a modified hybrid Stewart–Pyatt model [13]. The corresponding autoionizing states that are produced by electron-impact ionization of an inner-shell electron were also accounted for. Retaining such excited states is very important for a proper evaluation of the charge-state composition and, especially, the lineshapes of the inner-shell transitions, since the spontaneous radiative transitions of the inner-shell electrons between such states with an outer 'spectator' electron have energies that somewhat differ from that of the respective characteristic lines.

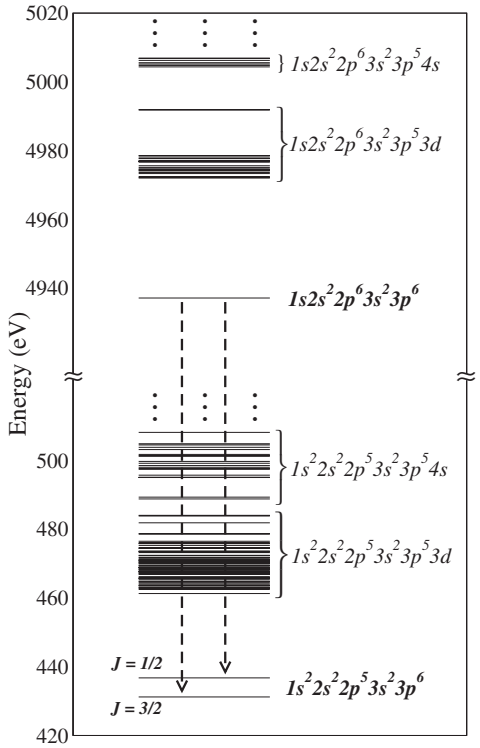

Figure 1. Part of the Ti VI inner-shell Grotrian diagram corresponding to the $K\alpha$ transition and its satellites.

The importance of these excited-state satellite transitions has been studied in the analysis of absorption and emission properties of dense aluminum [1, 4] and chlorine [3] plasmas. For higher-Z elements, satellite transitions due to holes in the M shell play a similar role [14].

For example, the energies of the Ti VI autoionizing states that give rise to the $K\alpha$ line and its satellites are shown in figure 1 (these are pure atomic data, with no plasma environment assumed). Radiative transitions between the $1s2s^22p^63s^23p^6$ and the two $1s^22s^22p^53s^23p^6$ states differing by the total angular momentum $J = 3/2$ and $1/2$ correspond, respectively, to the $K\alpha_1$ and $K\alpha_2$ components (designated by the dashed arrows). As seen from the diagram, the energies of the initial states with one of the outer electrons excited ($1s2s^22p^63s^23p^5nl$) are only ≈50 eV above the energy of $1s2s^22p^63s^23p^6$. Therefore, already at temperatures of 15–20 eV they should be significantly populated, and the $K\alpha$ shape modified because of the appearance of a multitude of $K\alpha$ satellites (not shown in the figure for the sake of clarity). In fact, this happens at even lower temperatures, as will be discussed below.

The natural line widths due to the radiative and autoionization decays were included in the calculations. For the Stark broadening, rates of all collisional processes included in the CR modeling were accounted for based on the theory of Baranger [15]. Since we operated with cross-sections and not amplitudes of the atomic processes, the contribution of the elastic parts of the process amplitudes was inevitably neglected. This omission, however, is believed to cause only minor inaccuracy, as will be discussed below. The Doppler broadening was also included, but is negligible for the bulk temperatures considered here (we assumed $T_i = T_e^{(\mathrm{bulk})}$).

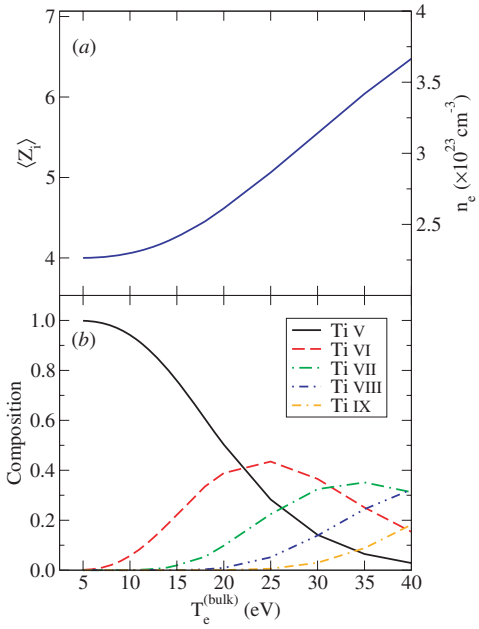

Figure 2. Electron density and mean ion charge (*a*) and charge-state distribution (*b*) in a solid-density titanium plasma as a function of the bulk electron temperature.

3. Results

Unless stated otherwise, in all calculations presented here the fast electrons are assumed to constitute a constant fraction of 0.1% of the total n_e, with a temperature $T_e^{(\mathrm{fast})} = 150$ keV. This choice is somewhat arbitrary, since no rigorous experimental data on the distribution of the fast electrons inside the target currently exist (see further on this problem in the discussion section). The electron density and the mean ion charge as a function of the bulk electron temperatures are shown in figure 2(*a*), while the charge-state distribution is given in figure 2(*b*). For the plasma conditions considered, only states with an excited electron in the 3d orbital survive the potential lowering; energies of the 4s-excited states (for all charge states included) already lie above the ionization threshold. The corresponding states with a vacancy in either K or L shell (e.g., $1s2s^22p^63s^23p^54s$ and $1s^22s^22p^53s^23p^54s$) were excluded from the calculations as well. It should be noted that the energies of some of the 4s-excited states are only slightly higher than the ionization threshold, therefore a more scrupulous approach would be to treat such states within the effective-statistical-weights model [16, 17], which is similar in spirit to using the Planck–Larkin renormalization of the partition function, as is done in [9]. However, the contribution of the 4s states to the lineshapes turned out to be very small. This was verified by running the calculations with and without including such states; the resulting $K\alpha$ spectra were practically indistinguishable.

Populations of the initial states of the Ti VI $K\alpha$ doublet and its satellites (relative to the population of the $1s2s^22p^63s^23p^6$ state) are given in figure 3 at three different bulk electron temperatures of 5, 10 and 15 eV. As seen, the populations of the excited states are rather close to the LTE values (for comparison, the Boltzmann exponents are shown by the dashed lines). Note that not only there are many $1s2s^22p^63s^23p^53d$ excited states, but their atomic

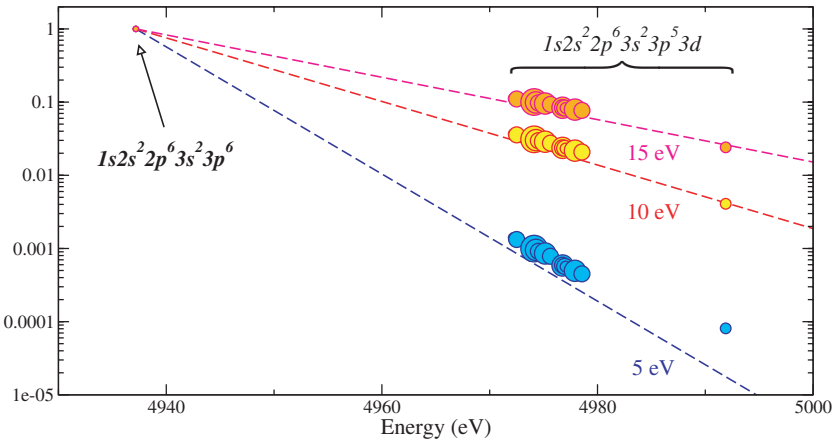

Figure 3. Relative populations of the Ti VI $1s2s^2\,2p^6\,3s^2\,3p^5$ nl states at different bulk temperatures. Symbol sizes are proportional to the atomic state degeneracy.

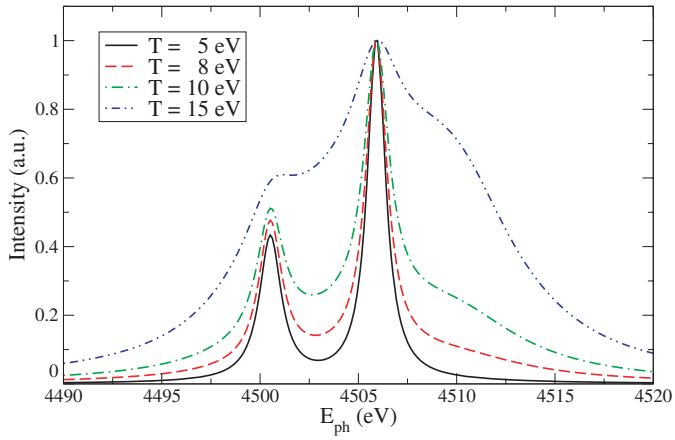

Figure 4. The Ti VI $K\alpha$ spectrum at different bulk temperatures. The spectra are peak-normalized.

degeneracy factors ($g = 2J + 1$, indicated by the symbol size in the figure) is, on average, significantly larger than the degeneracy of the $1s2s^22p^63s^23p^6$ state. As a result, these states begin to contribute to the $K\alpha$ lineshape at a relatively low temperature. This is demonstrated in figure 4, where Ti VI $K\alpha$ lineshapes at different bulk temperatures are shown. Indeed, the deviations from the 'cold' $K\alpha$ shape are noticeable already at 8 eV. At 10 eV, the lineshape is changed significantly, and at 15 eV[7], it is strongly asymmetric, the $K\alpha_1/K\alpha_2$ splitting is hardly seen, and the total spectrum is shifted on average to the higher energy region. This 'blue' shift of the excited-state satellites is similar to the relative shift of the next charge state, Ti VII. This is shown in figure 5, where a 'cold' (i.e., without the satellites) Ti VII $K\alpha$ spectrum is given for the comparison. The reason [1] of this similarity is that the excited 'spectator' electron

[7] Evidently, at this temperature the Ti VI $K\alpha$ spectrum does not represent the total Ti $K\alpha$ spectrum. As follows from figure 2(*b*), the $K\alpha$ radiation of the next charge state (Ti VII) contributes ≈20% of the total line intensity.

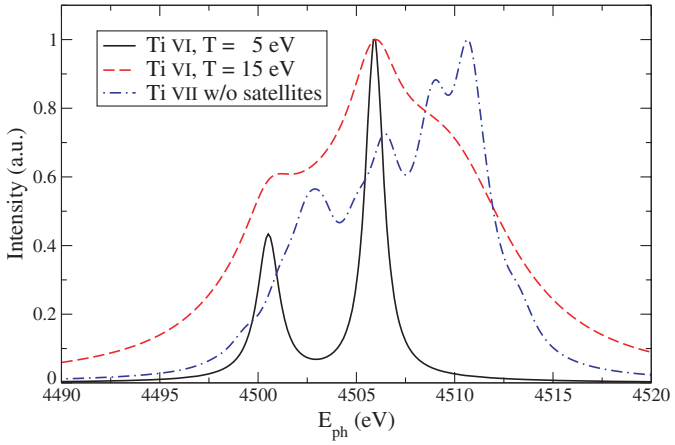

Figure 5. Ti $K\alpha$ spectra of neighbor charge states. With the bulk temperature increasing, the excited-level satellites cause the Ti VI $K\alpha$ spectrum to look qualitatively similar to the Ti VII $K\alpha$ emission without the satellites. The spectra are peak-normalized.

penetrates the inner shells relatively weakly, thus appearing to the inner-shell electrons almost like a free one.

We applied the calculations to preliminary data obtained in a recent experiment that was carried out at the Laboratoire pour l'Utilisation des Lasers Intenses (LULI) facility [18][8]. Here we provide a short description of the experimental setup, with details of the measurements and analysis to be published elsewhere [19]. A 10 μm titanium foil was irradiated by a 330 fs, 14 J laser pulse of 1057 nm wavelength, focused to a spot of $\approx$8 μm diameter, thus resulting in an intensity of about 9×10^{19} W cm^{-2} at the target surface. The laser hit the target at 11° to the surface normal. Single-shot spectra of the Ti $K\alpha$ doublet were recorded on a film using a toroidally bent GaAs crystal x-ray spectrometer with a resolving power of $E/\Delta E \approx 15\,000$ (corresponding to $\Delta E \approx 0.3$ eV at the Ti $K\alpha$ energy) and the spatial 1D resolution of $\approx$15 μm. The spectral resolution was not affected by the source size due to the use of the Johann configuration. The spectra were taken from the front side of the target, looking at 50° from the normal of the surface, thus integrating the spectra along the line of sight.

A $K\alpha$-emitting spot $\approx$250 μm in size was observed. A spectrum taken at the center of the 1D-imaged spot, integrated over a 45 μm-wide strip in order to enhance the signal-to-noise ratio, is presented in figure 6. A strong asymmetry of the spectrum is evident, with a tail extending to the 'blue' region (the cut-off at $\approx$4522 eV corresponds to the x-ray-crystal spectral-window edge).

The analysis of the measured spectrum unambiguously indicates a distribution of the bulk temperatures. Indeed, there is no way to explain the data assuming a single value of $T_e^{(\mathrm{bulk})}$. As seen in the figure, a temperature of about 14 eV is needed to make a good fit of the central part and the 'red' wing of the spectrum. However, the 'blue' wing of the spectrum calculated at this temperature is significantly below the measured one. On the other hand, a good fit of the 'blue' wing, requiring $T_e^{(\mathrm{bulk})} \approx 30$ eV (for which the spectrum is already dominated by $K\alpha$ radiation of higher Ti charge states, see figure 2(b)), is significantly shifted to the region of higher energies and has no resolvable structure of the $K\alpha_1/K\alpha_2$ doublet, both contradicting the experimental data. Thus, we are led to assume a distribution of the bulk temperatures which

[8] Laboratoire pour l'utilisation des lasers intenses http://www.luli.polytechnique.fr/.

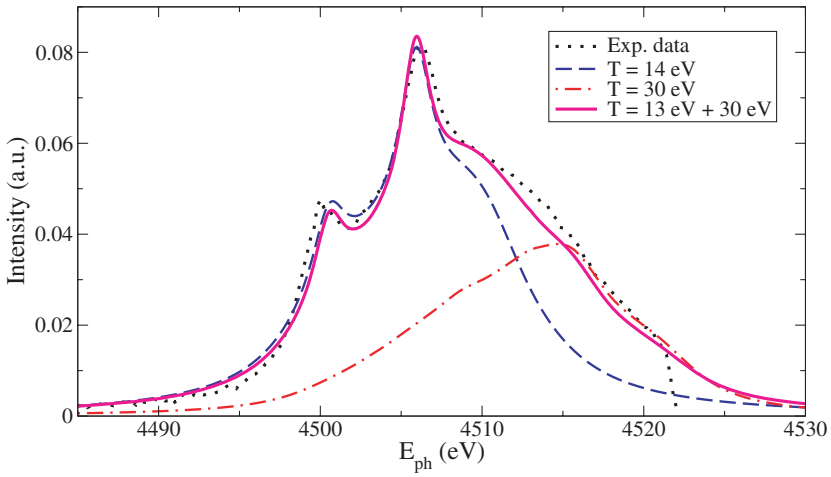

Figure 6. Experimental data, best single-bulk-temperature fits of the 'red' and the 'blue' wings and a synthetic spectrum with radiation from two regions with different temperatures assumed.

allows us to fit the data rather well. For example, a simple distribution of only two different values of $T_e^{(\mathrm{bulk})}$, 13 eV and 30 eV, taken with the weights of about 3/4 and 1/4, respectively, yields a synthetic spectrum that fits the data well, as seen in the figure. The reason for such a temperature distribution is the radial gradient of the plasma parameters (including $T_e^{(\mathrm{bulk})}$) along the line of sight. Another possibility is a change of the temperature over the duration of the $K\alpha$ emission. A work on re-constructing the radial dependence of the $K\alpha$ spectra and, thus, the radial profile of the bulk temperature is currently in progress [18].

4. Discussion

The very high electron density, $n_e \gtrsim 2.3 \times 10^{23}$ cm^{-3} (see figure 2(*a*)), corresponds to a rather high Fermi energy $E_F \approx 15$ eV, implying that the Fermi–Dirac statistical distribution needs to be used for the bulk plasma temperatures $\lesssim$15 eV. Nevertheless, the choice of the statistical distribution has almost no effect on the charge-state distribution even at such low temperatures. Indeed, only electrons with energies exceeding the ionization threshold ($\sim$100 eV for the Ti charge states considered) are responsible for ionization; however, such an energy significantly exceeds E_F, where both the Maxwell and Fermi–Dirac statistics give very close probabilities and, thus, similar ionization rates. Similarly, energy distances between levels connected by collisional transitions are at least several times larger than E_F. Notable exceptions of this rule are components of the same multiplet. In particular, the energy distance between the L_2 and L_3 shells (corresponding to the fine splitting between the 'cold' Ti $K\alpha_1$ and $K\alpha_2$ components) is only $\approx$6 eV. However, the collisional rates between these levels are relatively low, resulting, for $T_e^{(\mathrm{bulk})} \gtrsim 5$ eV, in the corresponding impact Stark widths of $\lesssim$0.1 eV, which is an order of magnitude less than the natural (due to the spontaneous radiation + Auger effect) width. Therefore, we believe that the choice of the distribution function should be largely unimportant for the Ti $K\alpha$ lineshape at the bulk temperatures considered in the present study.

Evidently, these arguments do not hold for the true 'cold' (i.e., x-ray tube) Ti $K\alpha$ spectra, where the quantum statistics and, in general, other solid-state phenomena should be very important. This might be the reason why the calculated energies and, especially, the widths of

$K\alpha_1$ and $K\alpha_2$ differ from the tabulated values [19]. To the best of our knowledge, there have been no theoretical studies explaining the 'cold' bulk Ti $K\alpha$ lineshape in an *ab initio* manner. In our calculations in the low-temperature limit the widths of $K\alpha_1$ and $K\alpha_2$ are, respectively, $\approx$1.1 eV and 1.2 eV, to be compared to the experimental 1.6 eV and 2.1 eV [20, 21]. For the $K\alpha_1$ energy and the $K\alpha_1/K\alpha_2$ splitting we obtained, using the FAC code, $\approx$4506 eV and 5.5 eV, respectively, to be compared with the experimental values of $\approx$4511 eV and 6 eV [20, 21]. We note that were the $K\alpha_1/K\alpha_2$ splitting corrected to the tabulated value, the calculated spectra in figure 6 would fit the measured data even better.

The plasma polarization shift is not an integral part of our CR calculations yet, but can easily be applied as a post-processor shifting the calculated spectra for each charge state appropriately. The $K\alpha$ polarization shift increases with $n_e^{(\mathrm{bulk})}$ but decreases with $T_e^{(\mathrm{bulk})}$ (see [9] for details). Since $\mathrm{d}n_e^{(\mathrm{bulk})}/\mathrm{d}T_e^{(\mathrm{bulk})}$ is positive (see figure 2(*a*)), the two dependencies partially cancel, resulting, for the plasma parameters considered here, in an almost constant 'red' shift varying by less than 1 eV.

Resonant self-absorption (opacity) effects can affect the $K\alpha$ lineshape significantly. For example, the optical depths τ at the peak of the strongest Al K-shell lines in intense proton-beam experiments [1] were inferred to vary from values below unity to those exceeding 10^3, depending on the target thickness. The opacity was accounted for in our CR calculations. Evidently, the effect depends strongly on the plasma dimensions and the energy distribution of the fast electrons inside the target, which are responsible for the creation of inner-shell holes. For the energy distribution of the fast electrons assumed (a Maxwellian distribution with a temperature of 150 keV and a density of 10^{-3} of the bulk n_e) we inferred $\tau \lesssim 0.1$ for the spectra presented in figure 6. With a higher fraction of the fast electrons the effect would evidently be more pronounced, resulting in somewhat lower inferred bulk temperature [1].

The dependence of the $K\alpha$ shape on the temperature of the fast electrons (or, more generally, on a specific form of their energy distribution) is rather weak as long as (i) the fast electrons represent a minor fraction of the total electron density, (ii) a majority of the fast electrons have energy significantly exceeding the *K*-edge limit ($\approx$5 keV for Ti) and (iii) the opacity is small. By varying $T_e^{(\mathrm{fast})}$ ten-fold in each direction we observed only minor changes in the shape of the emission spectra, albeit the total intensity changed by several times. This is because the lineshape is largely determined by the charge-state distribution, presence of the excited-state satellites, and their collisional broadening, where all these factors are only functions of the bulk electron temperature and density. The fast electrons, within the assumptions (i)–(iii) above, only determine the absolute populations of the atomic states. It is worth noting that, contrary to the particle-beam experiments, where the energetic particles are externally generated and thus their energy and density are well known, the energy, density and spatial distribution of the fast electrons *inside* the target in the intense laser–matter interactions cannot be measured directly. Part of the fast electrons with an energy sufficient to escape the target space charge form a beam that can be detected and its properties measured, see, e.g., [22]. However, these escaping electrons represent only a small fraction of the fast electrons inside the target. Based on absolute $K\alpha$ intensity measurements [23], this fraction amounts to about 10%. Preparations are currently under way for performing measurements aimed to infer the energy distribution of the fast electrons inside the target, based on intensity ratios of different inner-shell transitions.

5. Conclusions

Collisional-radiative calculations of solid-density laser-produced Ti plasma, with the inner-shell transition lineshapes modeled, were presented. Plasma polarization, ionization

potential lowering, Stark broadening, solid-density quantum effects and self-absorption were considered. In the calculations included were a large number of atomic states, including autoionizing states with inner-shell vacancies and an excited outer electron. The excited-state satellites of the $K\alpha$ transition have a rich structure that influences the $K\alpha$ lineshape already at rather low ($\sim$10 eV) bulk temperatures. Application of the modeling to the experimental data was successful, resulting in a distribution of the inferred bulk electron temperature.

Acknowledgments

We are grateful to D Salzmann, E Nardi, M Deutsch, S B Hansen, E Son and J Seely for fruitful discussions. This work was supported in part by the German-Israeli Foundation for Scientific Research and Development (GIF) and the USA DOE Center for High-Energy-Density Studies. YM is the incumbent of the Stephen and Mary Meadow Professorial Chair. HR and GR also acknowledge support by the DFG founded SFB 652.

References

[1] MacFarlane J J, Wang P, Bailey J, Mehlhorn T A, Dukart R J and Mancini R C 1993 Analysis of $K\alpha$ line emission from aluminum plasmas created by intense proton beams *Phys. Rev.* E **47** 2748–58
[2] Bailey J E, MacFarlane J J, Wang P, Carlson A L, Haill T A, Johnson D J, Lake P, McGuire E J and Mehlhorn T A 1997 Measurements of planar target heating by an intense lithium ion beam *Phys. Rev.* E **56** 7147–58
[3] Kawamura T, Horioka K and Koike F 2006 Potential of K[alpha] radiation by energetic ionic particles for high energy density plasma diagnostics *Laser Part. Beams* **24** 261–7
[4] Abdallah J, Clark R E H and Peek J M 1991 Excited-state 1s-2p absorption by aluminum ions with partially filled L shells *Phys. Rev.* A **44** 4072
[5] Mancini R C, Shlyaptseva A S, Audebert P, Geindre J P, Bastiani S, Gauthier J C, Grillon G, Mysyrowicz A and Antonetti A 1996 Stark broadening of satellite lines in silicon plasmas driven by femtosecond laser pulses *Phys. Rev.* E **54** 4147–54
[6] Kawamura T *et al* 2003 Numerical study of K[alpha] emission from partially ionized chlorine *J. Quant. Spectrosc. Radiat. Transfer* **81** 237–46
[7] Hansen S B *et al* 2005 Temperature determination using K alpha spectra from M-shell Ti ions *Phys. Rev.* E **72** 036408
[8] Chen S N *et al* 2007 Creation of hot dense matter in short-pulse laser–plasma interaction with tamped titanium foils *Phys. Plasmas* **14** 102701–6
[9] Sengebusch A, Reinholz H, Röpke G, Zastrau U, Kämpfer T, Uschmann I, Förster E, Stambulchik E, Kroupp E and Maron Y 2009 K-line emission profiles with focus on the self-consistent calculation of plasma polarization *J. Phys. A: Math. Theor.* **42** 214061
[10] Liberman D A 1982 INFERNO: a better model of atoms in dense plasmas *J. Quant. Spectrosc. Radiat. Transfer* **27** 335–9
[11] Ralchenko Yu V and Maron Y 2001 Accelerated recombination due to resonant deexcitation of metastable states *J. Quant. Spectrosc. Radiat. Transfer* **71** 609
[12] Gu M F 2003 Indirect x-ray line-formation processes in iron L-shell ions *Astrophys. J.* **582** 1241
[13] Murillo M S and Weisheit J C 1998 Dense plasmas, screened interactions, and atomic ionization *Phys. Rep.* **302** 1–65
[14] Chung H-K, Chen M H and Lee R W 2007 Extension of atomic configuration sets of the Non-LTE model in the application to the K[alpha] diagnostics of hot dense matter *High Energy Density Phys.* **3** 57–64
[15] Baranger M 1958 General impact theory of pressure broadening *Phys. Rev.* **112** 855
[16] Fisher D V and Maron Y 2003 Characterization of electron states in dense plasmas and its use in atomic kinetics modeling *J. Quant. Spectrosc. Radiat. Transfer* **81** 147
[17] Fisher D V and Maron Y 2002 Effective statistical weights of bound states in plasmas *Eur. Phys. J.* D **18** 93
[18] Zastrau U *et al* 2009 (in preparation)
[19] Deslattes R D, Kessler E G, Indelicato P, Billy L de, Lindroth E and Anton J 2003 X-ray transition energies: new approach to a comprehensive evaluation *Rev. Mod. Phys.* **75** 35–99
[20] Bearden J A 1967 X-ray wavelengths *Rev. Mod. Phys.* **39** 78

[21] Anagnostopoulos D F, Gotta D, Indelicato P and Simons L M 2003 Low-energy x-ray standards from hydrogenlike pionic atoms *Phys. Rev. Lett.* **91** 240801
[22] Hidding B *et al* 2007 Novel method for characterizing relativistic electron beams in a harsh laser-plasma environment *Rev. Sci. Instrum.* **78** 083301
[23] Zamponi F 2007 Electron propagation in solid matter as a result of relativistic laser plasma interactions *PhD Thesis,* Friedrich-Schiller-Universität, Jena, Germany